Isomerization Behavior of an Azopolymer in Terms of the Langmuir−Blodgett Film Thickness and the Transference Surface Pressure

Marta Haro, Beatriz Giner, Ignacio Gascón, Félix M. Royo, and M. Carmen López*

Departamento de Química Orgánica-Química Física, Facultad de Ciencias, Plaza de San Francisco, Ciudad Universitaria, 50009 Zaragoza, Spain

Received October 26, 2006; Revised Manuscript Received December 19, 2006

ABSTRACT: The photoinduced trans−cis and thermal cis−trans isomerizations of an azopolymer were investigated in terms of LB film thickness and the transference surface pressure by means of UV−vis spectroscopy and AFM microscopy. Three different photochemical behaviors have been observed depending on the number of layers: (i) for 1 layer, the percentage of cis isomers in the photostationary state is around 25%, (ii) in films of 5−20 layers, this percentage decreases to ca. 15%, and (iii) for 35 layers, the percentage of isomers cis formed after irradiation is more than 50%. Furthermore, the thermal cis−trans isomerization varies from a first-order kinetics to an expression with two exponential terms when the LB films change from 1 layer to multilayers. Morphologic changes in the surface of the films during the photoisomerization process were observed by means of AFM, and these changes also depend on the number of layers. In the cis state some hills were observed in the films of 1 and 35 layers, whereas practically no changes occurred in the films of 10 layers. These hills can be interpreted as the rupture of bidimensional structure of the film during the photoisomerization process. Three different schemes have been proposed to explain the observed behaviors.

1. Introduction

Azoaromatic dyes are very promising photochromic materials for their potential optoelectronic and photonic applications.[1] Most of their applications are directly or indirectly related with the reversible trans−cis−trans photoisomerization of the azobenzene group, such as optical information storage,[1,2] light switching devices,[3] surface relief gratings,[4] holograms,[5,6] and induction of liquid-crystals alignment.[7,8] The photoisomerization process has been investigated extensively due to both practical and theoretical interest.[9−12] In particular, polymers functionalized with azobenzenes (azopolymers) are very attractive since they are thermically and mechanically more stable than their respective monomers and they are the preferred choice for thin film fabrication.[13] Since film structure affects the photoisomerization and the optical storage properties of azobenzene materials, several molecular engineering strategies have been used to optimize both order and thickness of thin films of azopolymer materials.[14] Between these methods, Langmuir−Blodgett (LB) and self-assembly (SA) can provide a high degree of control.[15] The LB technique allows the transference of the desired number of layers from the air−water interface to a solid substrate, maintaining a high order in each layer.

The photoisomerization efficiency and kinetics of an azopolymer in a LB film differ from reaction in solution due to the different freedom of chromophores mobility. The trans−cis photoisomerization is accompanied by an increase of area because *cis*-azobenzene has a larger cross section than *trans*-azobenzene. Therefore, free volume around the chromophores should exist in order for the reaction to occur. Free volume means not only that there are actual voids but also that additional space can be created easily. Consequently, when there is enough free volume, photoisomerization will proceed, whereas if the molecules are closely packed in the film, they will not photoisomerize. When the chromophores align themselves into an ordered structure such as the case of LB films, photoisomerization is hindered since it would destroy the intrinsic order. Therefore, in LB films it has been extensively accepted that all the processes related with photoisomerization should occur two-dimensionally,[16−19] and consequently free volume in each layer in the LB films should be necessary for photoisomerization because the cross section of the molecules increases during the reaction.

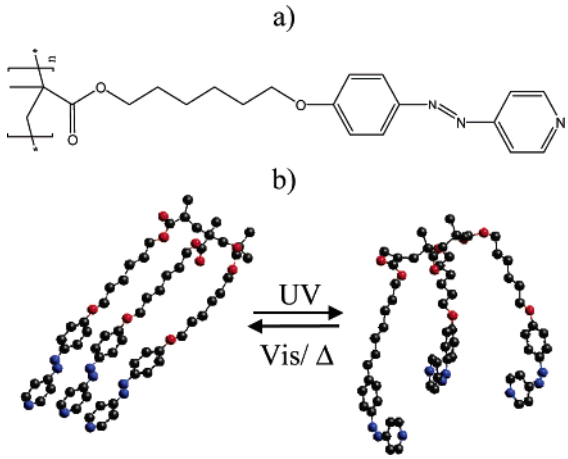

Figure 1. Molecular structure of PAzPy (a). PAzPy photoisomerization model (b), where the three lateral branches represented were optimized in the trans and cis form by using the conjugated gradient Newton−Raphson algorithm in molecular mechanics (MM+ by Allinger).

Nevertheless, morphological changes in azobenzene surface films during photoisomerization have been reported by means of AFM.[20−23] Matsumoto et al.[24] in 1998 showed that these morphological changes were reversible by alternate illumination in LB films, indicating that three-dimensional structures are involved, and then the concept of free volume does not hold in that case. Since three-dimensional structures

* To whom correspondence should be addressed: e-mail mcarmen@unizar.es, phone + 34 976 76 11 96, fax + 34 976 76 12 02.

10.1021/ma0624752 CCC: $37.00
Published on Web 02/13/2007

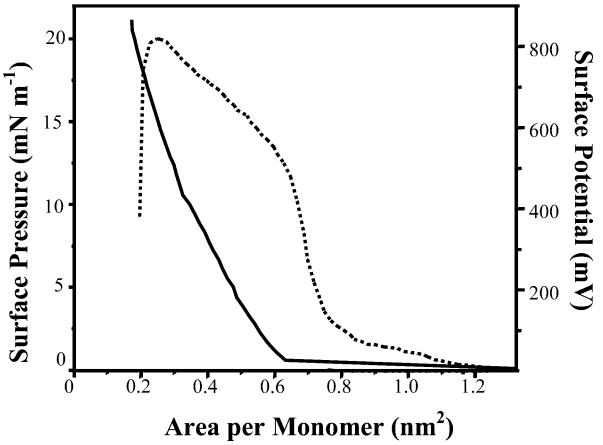

Figure 2. $\pi-A$ (—) and $\Delta V-A$ (- - -) isotherms of PAzPy recorded at 20 °C.

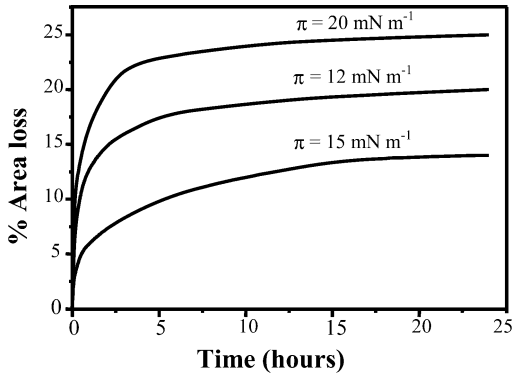

Figure 3. Percentage of area loss vs time when the surface pressure is maintained at a constant surface pressures of 12, 15, and 20 mN m^{-1}.

are involved in photoisomerization processes, free volume should exist not only inside the layers but also in all the structure of thin films.

The aim of this paper is to relate the percentage of isomers cis in the photostationary state and the thermal cis−trans kinetics of an azopolymer with the number of layers and transference surface pressure (π_{tr}, related to chromophore surface density) of the LB film. To achieve this purpose, several azopolymer LB films with different number of layers and the surface density of chromophores were fabricated. After checking the quality of the obtained LB films (IR and UV−vis spectroscopy and optical microscopy), isomerization processes (both trans−cis and cis−trans) were monitored by means of UV−vis spectroscopy and AFM. The polymer selected is an azopolymer of lateral chain (briefly called PAzPy, Figure 1a), with electron-donor (O ether) and electron-acceptor (N pyridine) substituents. This structure favors a quick trans−cis−trans isomerization and, consequently, the photoinduced orientation.[1] Moreover, the pyridine group is hydrophilic and can interact with the water surface in the Langmuir films and with the hydrophilic substrates to give good Langmuir−Blodgett films, as we have observed previously.[25]

2. Experimental Details

The synthesis of PAzPy was described in a previous paper.[25] The molecular weight of the polymer-repetitive unit (367 g mol^{-1}) was adopted for molar concentration and all area calculations.

Films were prepared at 20 ± 1 °C using a 210 × 460 mm^2 homemade Teflon trough described elsewhere.[26] The subphase was Millipore Milli-Q water (resistivity 18.2 MΩ cm). PAzPy was dissolved in chloroform HPLC grade (99.9%) provided by Aldrich,

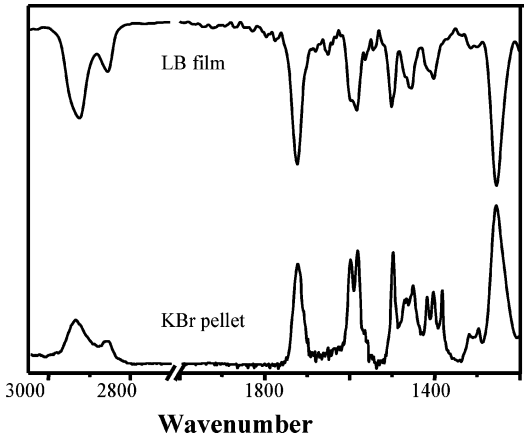

Figure 4. IR spectra of PAzPy in LB film (35 layers transferred at 15 mN m^{-1}) and in KBr pellet.

Table 1. Infrared Band Centered in Wavenumber (cm^{-1}), Relative Intensities, and Normal Mode Assignments

KBr pellet		LB film		
wave-no.	rel int	wave-no.	rel int	assignment
1253	vs	1249	vs	ring stretching + C−H bend in chain
1404	m	1404	m	H−C−H scissoring
1454	s	1457	s	H−C−H scissoring in chain
1500	s	1501	s	H−C−H scissoring + C−H bend in plane
1584	s	1586	vs	pyridine ring stretch
1602	s	1598	s	ν phenyl ring stretch
1725	s	1723	vs	C═O stretching
2864	w	2855	m	CH_2 stretch symmetric
2935	w	2928	s	CH_2 stretch asymmetric

and a 5×10^{-5} M solution was spread onto the water surface to fabricate the Langmuir films. A method of successive cycles of spreading, compressing, and decompressing, previously used to obtain homogeneous and stable Langmuir films,[27] has been employed: 1 mL of the polymer solution was spread, and after compression and decompression processes, another amount of solution (0.5 mL) was added onto the water surface. The whole process was repeated until the total required volume (2.5 mL) was spread. The last compression was performed at 4 mm min^{-1}, whereas for the other film compressions a barrier speed of 12 mm min^{-1} was used.

Langmuir films were transferred onto solid substrates by the vertical dipping method at a constant surface pressure of 12, 15, and 20 mN m^{-1} with a lifting speed of 7 mm min^{-1}. The obtained LB films were Z-type,[25] with the first layer transferred on the up trip. Depending on the nature of the experiment, several solid substrates were employed: CaF_2 (IR spectroscopy), quartz (UV−vis spectroscopy), silver islands films (optical microscopy), and mica (atomic force microscopy, AFM). More details concerning the cleaning procedure of the substrates and the preparation conditions have been reported before.[28−30] Silver island films of 9 nm mass thickness were prepared in a Balzers BSV 080 glow discharge evaporation unit. Metal films were deposited on preheated (200 °C) glass (7059 Corning) and KRS-5 (Aldrich) slides. During film deposition, the background pressure was maintained at 10^{-6} Torr, and the average deposition rate (0.5 Å s^{-1}) was monitored using an XTC Inficon quartz crystal oscillator.

The $\Delta V-A$ measurements were carried out using a Kelvin probe provided by Nanofilm Technologie GmbH, Göttingen, Germany.

The transmission IR spectra were recorded with a Jasco 410 Fourier transform IR spectrometer. UV−vis spectra of PAzPy solution and LB films were carried out using a Varian Cary 50 UV−vis spectrophotometer. Optical microscopy images were obtained with a Leica microscope (DMLM). The AFM experiments were performed by means of a multimode extended microscope

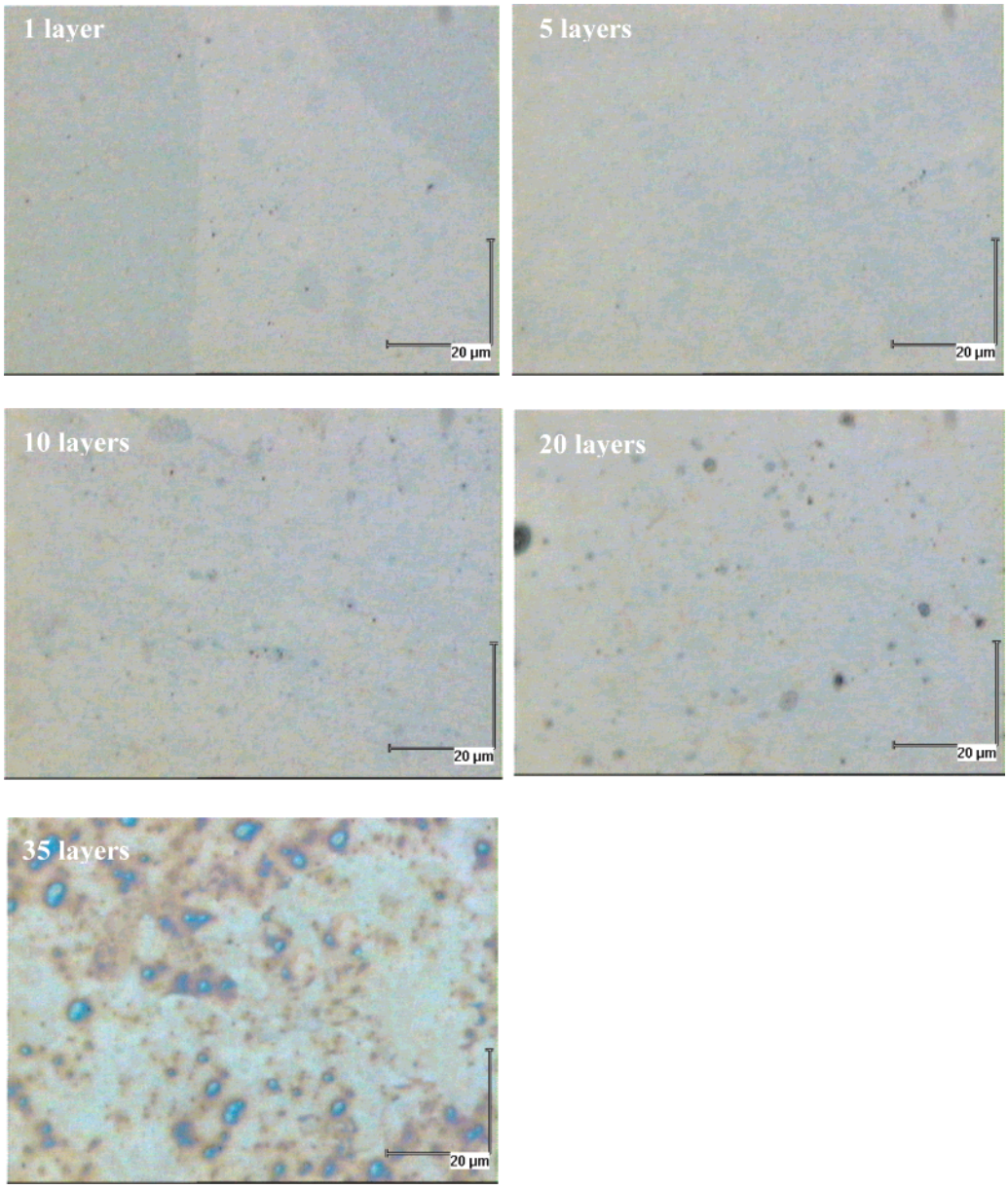

Figure 5. Optical microscopy images of LB films of 1, 5, 10, 20, and 35 layers transferred at 15 mN m^{-1}.

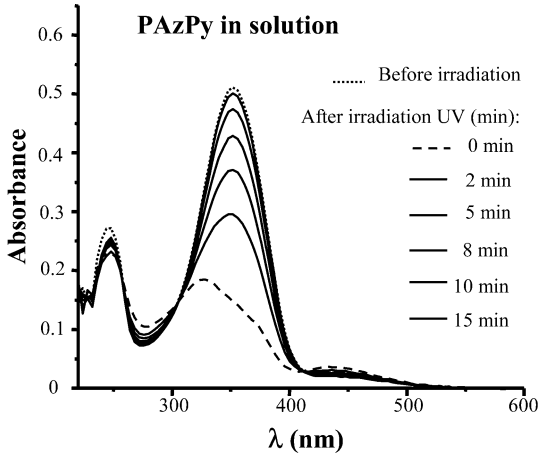

Figure 6. UV−vis spectra of PAzPy in 1,2-dimethoxyethane (3.5×10^{-5} M) before and after UV irradiation (365 nm) and during the thermal cis−trans isomerization.

with Nanoscope IIIA electronics from Digital Instruments, using the tapping mode.

Table 2. Apparent Extent of Photoisomerization, Y_{app}, at the Photostationary State of PAzPy in Solution and in the LB Films of Different Thickness and Surface Density of Chromophore Units

	PAzPy in solution (3.5×10^{-5} M) 0.82				
	PAzPy in the Langmuir−Blodgett films				
	1 layer	5 layers	10 layers	20 layers	35 layers
12 mN m^{-1}	0.20	0.07	0.17	0.18	0.53
15 mN m^{-1}	0.27	0.05	0.21	0.20	0.63
20 mN m^{-1}	0.31	0.07	0.21	0.21	0.65

The photoisomerization of PAzPy in solution (in a quartz cell of 1 cm light path with Teflon top provided by Hellma) and in the LB films was induced by illumination with a monochromatic Xe UV lamp (at 365 nm) of 1000 W cooled with water, from Oriel Universal.

3. Results

Figure 1 shows the molecular structure of PAzPy and the trans−cis−trans isomerization model, where both PAzPy isomers (trans and cis, represented only with three branches) were geometrically optimized by using the conjugated gradient Newton−Raphson algorithm in molecular mechanics (MM+

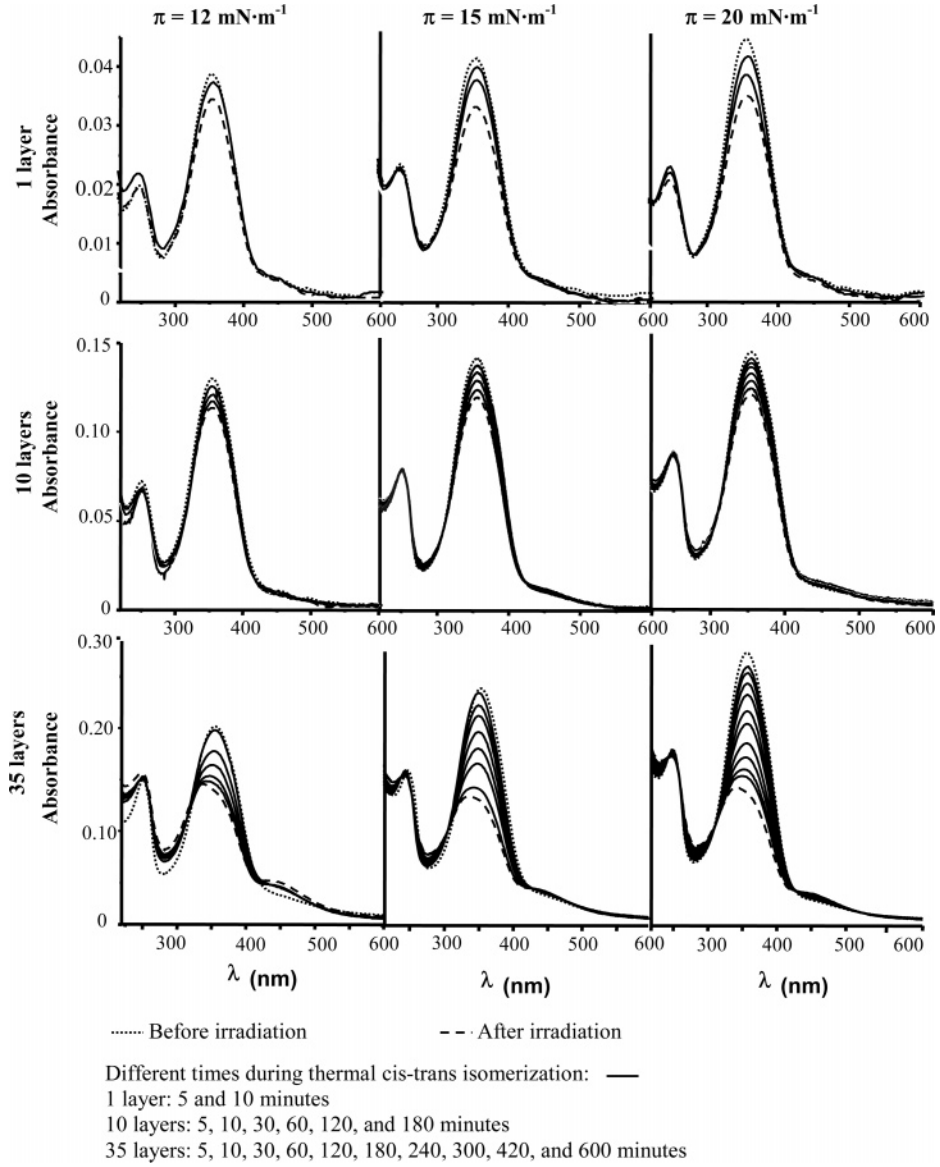

Figure 7. UV−vis spectra of PAzPy in LB films of 1, 10, and 35 layers transferred at 12, 15, and 20 mN m^{-1}, before and after UV irradiation (365 nm) and during the thermal cis−trans isomerization.

Table 3. Thermal Cis−Trans Kinetic Parameters of PAzPy in Solution and in the LB Films of Different Number of Layers and Transference Surface Pressure

	PAzPy in solution (3.5×10^{-5} M) k (min^{-1}) 0.22								
	Langmuir-Blodgett films								
	π = 12 mN m^{-1}			π = 15 mN m^{-1}			π = 20 mN m^{-1}		
layers	α	k_1 (min^{-1})	k_2 (min^{-1})	α	k_1 (min^{-1})	k_2 (min^{-1})	α	k_1 (min^{-1})	k_2 (min^{-1})
1	1	0.25		1	0.16		1	0.12	
5	0.31	0.25	0.022	0.53	0.16	0.018	0.56	0.12	0.016
10	0.20	0.25	0.022	0.38	0.16	0.011	0.18	0.12	0.007
20	0.18	0.25	0.013	0.26	0.16	0.011	0.15	0.12	0.006
35	0.15	0.25	0.012	0.11	0.16	0.009	0.12	0.12	0.004

by Allinger).[31] In this figure we can realize that photoisomerization of azobenzene units modifies the whole polymer.

3.1. Langmuir and Langmuir−Blodgett Films. The LB technique originally designed for amphiphilic materials provides ordered molecular structures both at the air−water interface and on solid substrates. For polymeric materials ordered structures are unlikely to be formed since one has little control over the molecular packing, but the LB technique can still provide a high degree of control of film thickness and surface uniformity if conditions for deposition are optimized. The film characterization by several techniques indicates that the Langmuir and LB films preparation method used is adequate. In this section, we show the more relevant results for a better discussion of the photoisomerization process.

Figure 2 shows the $\pi-A$ isotherm of PAzPy film, featuring a liftoff area of 0.65 nm^2 per monomer, and a liquid-expanded region up to 4 mN m^{-1} at 0.5 nm^2. Upon further compression, the pressure increases more steeply up to 11 mN m^{-1}. After this slope change, the films were deposited at three different transference surface pressures, π_{tr}: 12, 15, and 20 mN m^{-1}

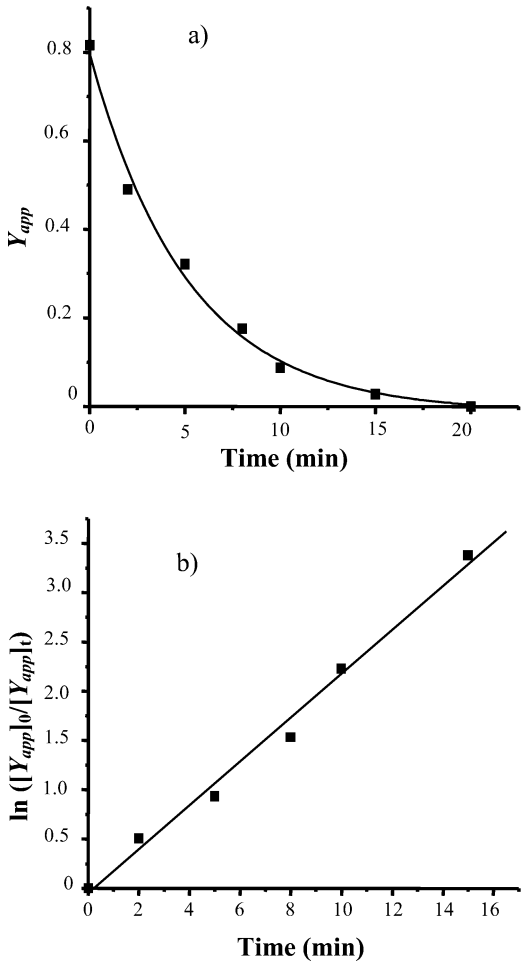

Figure 8. Y_{app} (a) and ln([Y_{app}]$_0$/[Y_{app}]$_t$) (b) vs time, *t*, during the thermal cis−trans isomerization of PAzPy in solution.

which correspond to 0.30, 0.25, and 0.18 nm^2, respectively. The theoretical area per azobenzene unit disposed vertically with an orientation of the transition dipole moment normal to the water surface onto the water surface is $A_{azobenzene} = 0.245$ nm^2.[32] This value is in good agreement with the area per monomer at 15 mN m^{-1} where a well-packed structure is expected. At 12 mN m^{-1} the area per monomer unit is a bit greater, and then the molecular structure can be more relaxed than at 15 mN m^{-1}. At 20 mN m^{-1}, the physical area per monomer is slightly smaller than the theoretical value, and some defects can be formed probably due to the ejection of some lateral branches of the polymer from the Langmuir film. The $\Delta V-A$ isotherm (Figure 2, dashed line) shows a drastic decrease in the surface potential at an area per monomer of 0.24 nm^2, indicative of azobenzene unit orientation change at the air−water interface. This result suggests that a different molecular organization exists at 0.18 nm^2 (surface pressure of 20 mN m^{-1}) than at 0.25 and 0.3 nm^2 (surface pressures of 15 and 12 mN m^{-1}, respectively), being the molecules more tilted onto the water surface at 20 mN m^{-1}, or some azobenzene units ejected from the Langmuir film; therefore, some three-dimensional structures can coexist with the Langmuir film.

Figure 3 shows the percentage of area loss when the surface pressure is maintained at the three π_{tr}. The greatest stability of the Langmuir film is reached at 15 mN m^{-1}, whereas at 12 mN m^{-1} is slightly lower and the area loss is practically twice when the surface pressure is 20 mN m^{-1}. This result supports the above-mentioned hypothesis of a well-packed structure at 15 mN m^{-1} and a reorganization of molecules at 20 mN m^{-1} giving a more disordered and unstable monolayer.

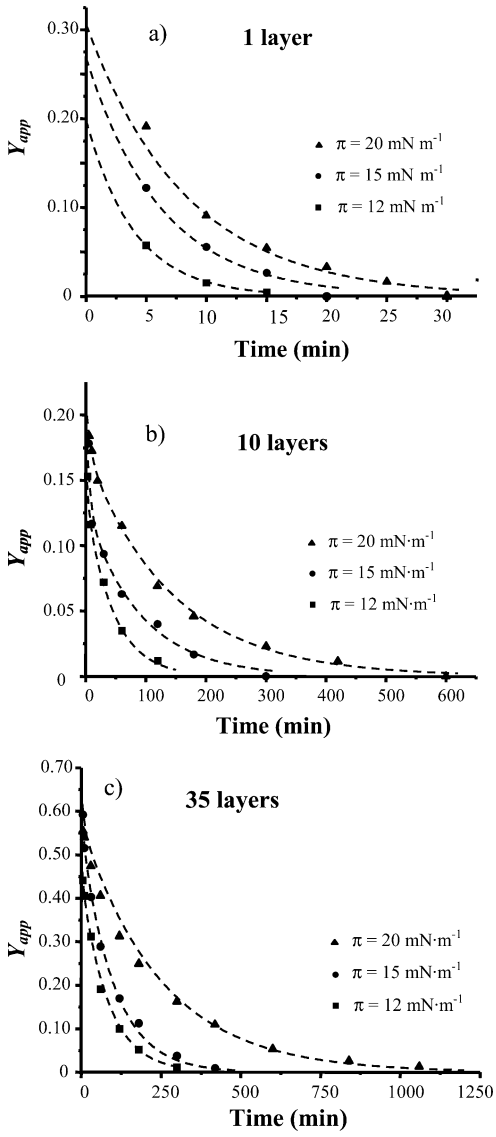

Figure 9. Y_{app} vs time, *t*, during the thermal cis−trans isomerization of PAzPy in the LB films of 1 (a), 10 (b), and 35 (c) layers transferred at 12, 15, and 20 mN m^{-1}. Dotted lines have been obtained with eq 3.

The IR spectra of PAzPy in LB film (35 layers transferred at 15 mN m^{-1}) and bulk solid face in a pressed KBr matrix are collected in Figure 4. Characteristic vibrational modes are listed in Table 1, including the assignments and the corresponding observed values in the LB film and in the pellet. There are some differences between the IR spectra of the azopolymer in an ordered structure such as the LB film and in a KBr pellet. The bandwidth in general increases in the LB film in the region of 1200−1800 cm^{-1}, probably due to more chromophore unit density, causing overlapping of multiple bands with slightly shifted frequencies. The IR gives important information about conformational order and packing of the alkyl chains. The $\nu_a(CH_2)$ and $\nu_s(CH_2)$ bands displaced 7 and 9 cm^{-1}, respectively, to lower wavenumber when the polymer is in the LB film with respect to the bulk solid face in a pressed KBr matrix. This phenomenon is indicative of relatively ordered alkyl chains with a trans zigzag conformation in the LB film.[33,34]

Figure 4 shows the optical microscopy images of the LB films of 1, 5, 10, 20, and 35 layers transferred at 15 mN m^{-1}. The

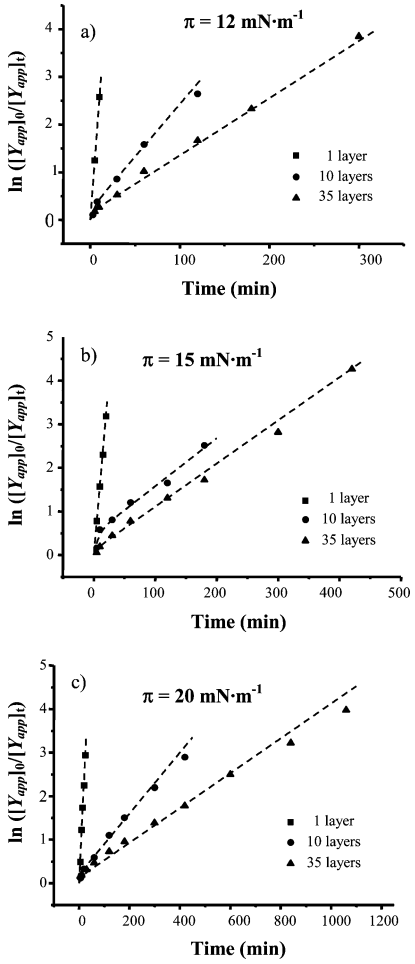

Figure 10. $\ln([Y_{app}]_0/[Y_{app}]_t)$ vs time, t, during the thermal cis−trans isomerization of PAzPy in the LB films of 1, 10, and 35 layers transferred at 12 (a), 15 (b), and 20 (c) mN m^{-1}. Dotted lines have been obtained with eq 3.

films look very homogeneous in the first depositions (i.e., 1 and 5 layers). In the films of 10 and 20 layers the surfaces are quite homogeneous with some defects of the film, presumably produced during the transference process. The defects increase with the number of transferences as it is clearly observed in the 35 layer film. In this film some domains where the structural order has been lost are observed.

3.2. Photoisomerization. UV−Vis Spectroscopy. To examine the trans−cis−trans processes of PAzPy in terms of LB film thickness and transference surface pressure, 1, 5, 10, 20, and 35 layers of PAzPy were transferred from the air−water interface to quartz substrates at 12, 15, and 20 mN m^{-1}. The surface pressure of transference determines the surface density of azobenzene units in a layer. Photochemical trans−cis isomerization and thermal cis−trans reverse isomerization were investigated by UV−vis spectroscopy and compared with a dilute solution of PAzPy in 1,2-dimethoxyethane (3.5×10^{-5} M). In this state (dilute solution) the isomerization depends on the azopolymer nature and can help us to discuss the obtained results in the films.

The photoisomerization of the azopolymer from the trans form to the cis one was induced by irradiation with ultraviolet light (365 nm). Figures 6 and 7 show the absorption spectra of the polymer in dilute solution and in the LB films of 1, 10, and 35 layers transferred at the three different surface pressures, respectively. We do not show the UV−vis spectra obtained for the LB films of 5 and 20 layers for shortening purposes; nevertheless, the results will be analyzed with the other films. Dotted lines represent the electronic absorption of PAzPy before irradiation. Two strong absorption bands attributed to $\pi-\pi^*$ electronic transition are observed. The absorption band located around 258 nm is attributed to a transition dipole moment along the short axis of the azobenzene chromophore. The long axis transition at lower photoexcitation energy at 354 nm is strongly affected by the chemical structure of azopolymer.[35] This peak appears at same λ in the LB films and in the solution, indicating that the electronic structure of the chromophore is not altered in the solid phase of the LB film. Furthermore, a weak band around 450 nm can be observed as a shoulder of the $\pi-\pi^*$ band, which is ascribed to the $n-\pi^*$ electronic transition. This photochemical behavior corresponds to an aminoazobenzene according to Rau's classification.[9] Broken lines represent the electronic absorption of PAzPy after irradiation. Figure 6 shows the shift down of the $\pi-\pi^*$ band from 354 to 327 nm, corresponding to the maximum absorbance of trans and cis isomers, respectively. In Figure 7, we can see that the change of UV−vis spectra of PAzPy in LB films, before and after irradiation, depends on the number of layers and π_{tr}. Solid lines show UV−vis spectra during the thermal cis−trans isomerization at 20 °C.

The photostationary state was achieved within 10 min of irradiation for all the samples, except for the monolayer films that needed only 5 min of irradiation. The apparent extent of photoisomerization (i.e., disappearance of the trans isomer) can be determined by[36]

$$Y_{app} = \frac{A_{trans} - A_t}{A_{trans}} \quad (1)$$

where A_{trans} and A_t correspond to absorbance at 354 nm (λ_{max} for the $\pi-\pi^*$ transition of the trans form) of the unirradiated (considering that 100% of molecules are in trans form) and irradiated states, respectively. Y_{app} in the photostationary state calculated for all samples are summarized in Table 2. These values should be considered only as approximated ones because the UV−vis spectra cannot be measured at the same time as the irradiation of the samples, and consequently, some cis molecules have isomerized to trans form when the UV−vis were performed. (This effect is especially important in the 1-layer films where the cis−trans kinetics is fast, as will be seen below.) Nevertheless, for a qualitative discussion these values are very useful.

As was expected, Y_{app} of PAzPy in the photostationary state is greater in solution than in LB films, probably due to smaller free volume in the solid matrices compared with that in solution. With respect to the film thickness the results are quite interesting. The value of Y_{app} decreases from 1 as the number of layers increases, as can be seen in the film of 5 layers, where the obtained percentage of cis isomers in the photostationary state is very small. The apparent extent of photoisomerization increases slightly with the number of layers deposited until 20; nevertheless, in all these films, Y_{app} is smaller than the obtained values for the monolayer films. A huge increase of the percentage of trans isomers that can isomerize is produced when the film thickness increases from 20 to 35 layers. Furthermore, in the films of 1 and 35 layers Y_{app} in the photostationary state increases slightly with the surface pressure of transference; meanwhile, in the films of intermediate thickness the obtained values are quite similar. The increase of Y_{app} values in the photostationary state with the π_{tr} can be due to cooperative motions between azobenzene moieties, as has been described before in LB films.[1]

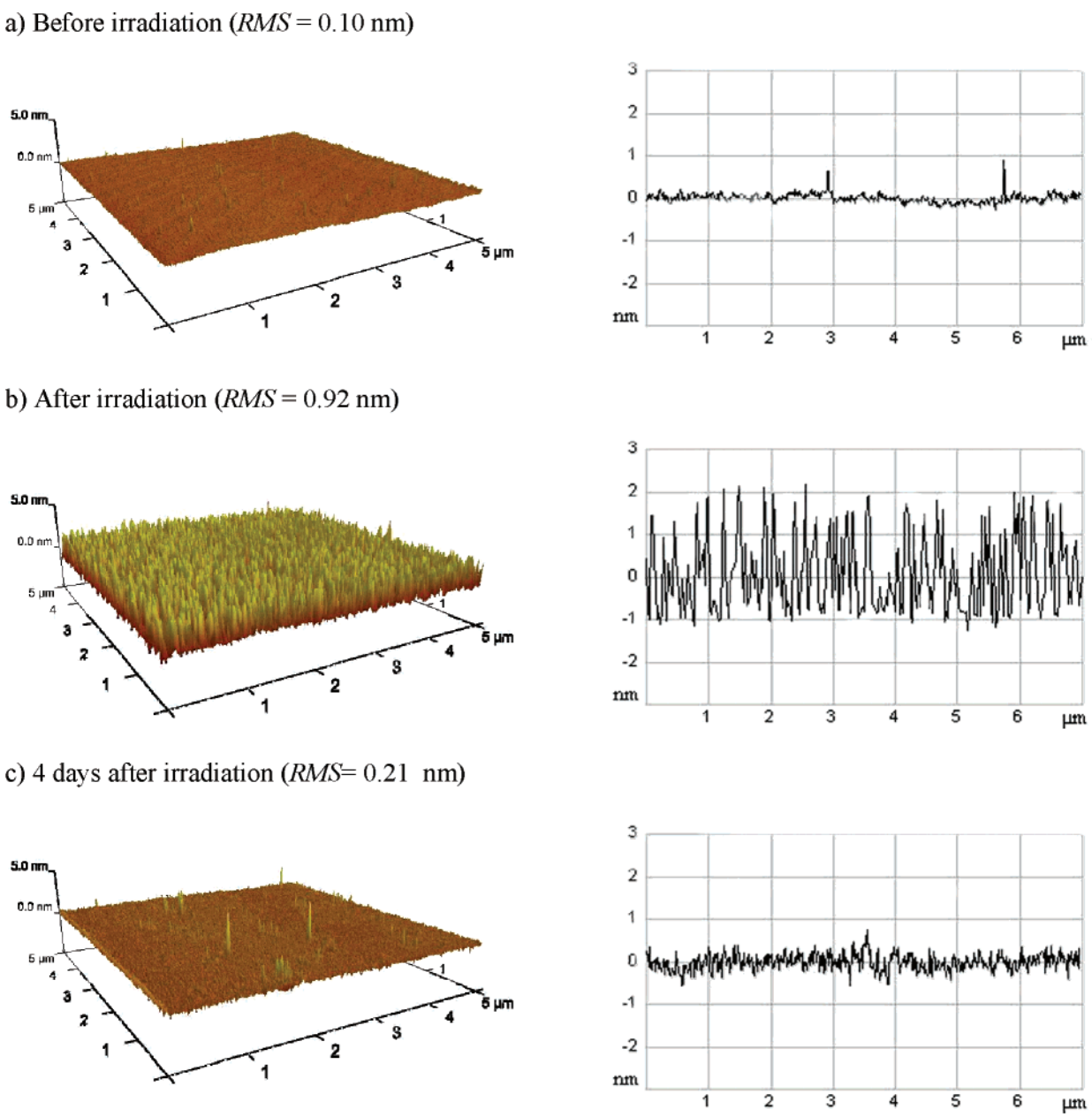

Figure 11. 3D and section analysis AFM images of the one-layer film transferred at 15 mN m^{-1}: (a) before irradiation with UV light (365 nm), (b) after irradiation, and (c) 4 days after the irradiation process.

After photoisomerization, the samples were left to isomerize thermally from cis to trans form. During this process, three distinct isosbestic points at 310, 430, and 490 nm can be observed in all samples. This phenomenon indicates that only two absorbing species (trans and cis isomers) are present, and no side reactions such as photocross-linking or photodegradation occurs. The evolution of this process can be monitored by the representation of Y_{app} vs time. Figure 8a shows Y_{app} vs time of PAzPy in solution. The cis molecule's lifetime is around a few minutes, which agrees with aminoazobenzene behavior. The experimental points can be fitted to an exponential function of first-order that suggests first-order kinetics for the process of thermal isomerization:[37]

$$\ln\left(\frac{[Y_{app}]_0}{[Y_{app}]_t}\right) = kt \qquad (2)$$

where $[Y_{app}]_0$ and $[Y_{app}]_t$ are apparent extent of photoisomerization isomers in the photostationary state ($t = 0$) and after a time t (min). The plot of $\ln([Y_{app}]_0/[Y_{app}]_t)$ vs time, t, is illustrated in Figure 8b. The slope of the lineal regression corresponds to the kinetic constant, whose value is indicated in Table 3.

Figure 9 shows Y_{app} vs time, t, for the LB films of 1, 10, and 35 layers at the three surface pressures of transference. It can be observed that the lifetime of cis isomers increases with the number of layers and the surface pressure of transference. The lifetime of cis isomers increases until hours in the case of multilayer films. This effect can be explained if cis isomers have stronger interactions with the surrounding matrix than trans isomers. This proposal was suggested previously[38,39] to interpret the fact that some films hardened after being irradiated. Under this assumption, the thermal cis−trans isomerization kinetics can be explained to be slower with the increase of the layer number and the chromophore surface density of the LB films since these two factors favor attractive interactions between molecules.

Figure 10 shows the plot of $\ln([Y_{app}]_0/[Y_{app}]_t)$ vs time, t, of the LB films with 1, 10, and 35 layers transferred at 12, 15,

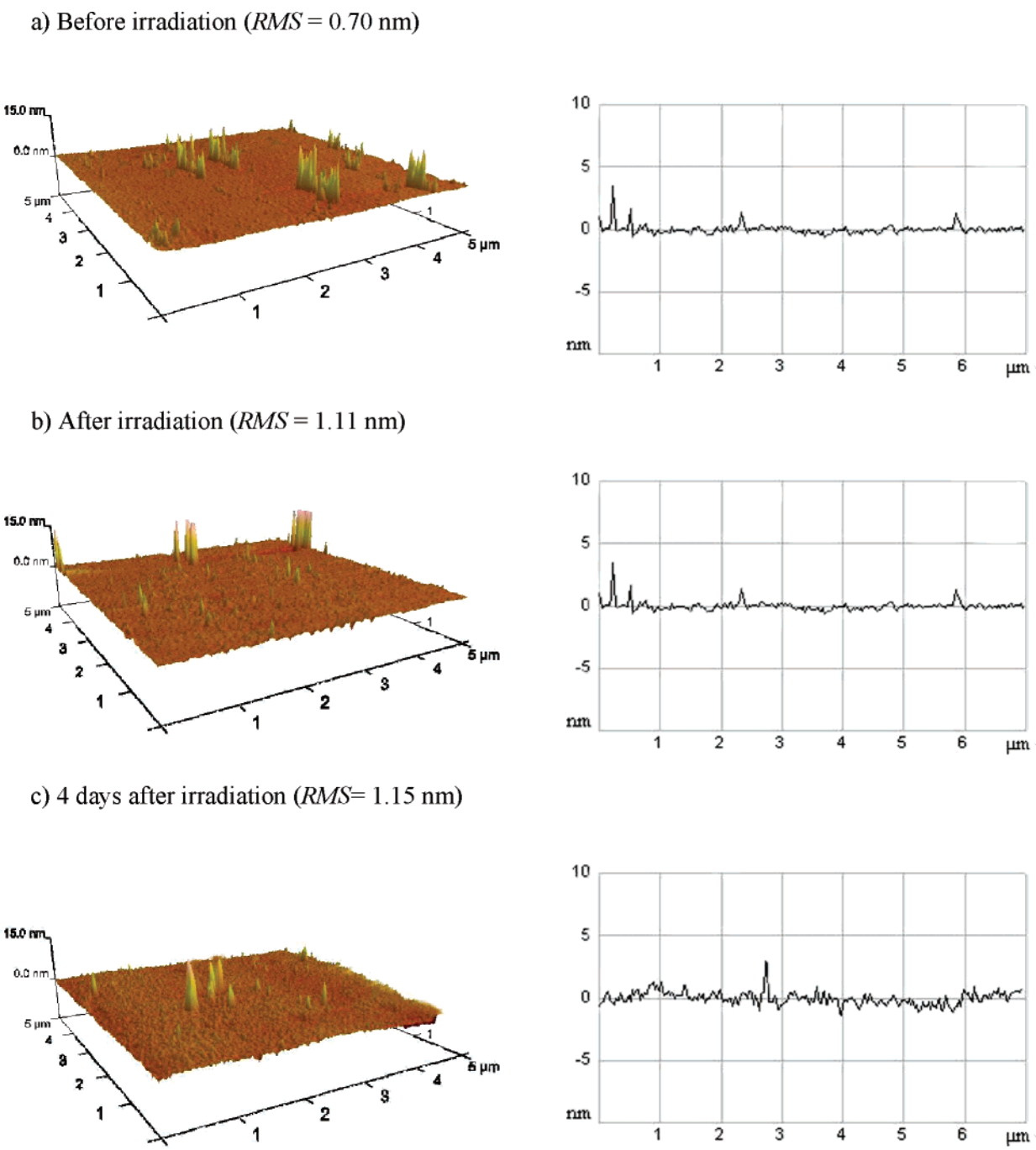

Figure 12. 3D and section analysis AFM images of the 10-layer film of transferred at 15 mN m^{-1}: (a) before irradiation with UV light (365 nm), (b) after irradiation, and (c) 4 days after the irradiation process.

and 20 mN m^{-1}. In this figure it is shown that the monolayer films follow a kinetics of first-order in the process of thermal cis−trans isomerization, independently of the π_{tr}. Therefore, the slope of the lineal regression corresponds to the value of the kinetic constant. The obtained values are shown in Table 3. In the case of multilayer films, the representation of $\ln([Y_{app}]_0/[Y_{app}]_t)$ vs time, t, deviate from a first-order kinetics. This behavior was previously observed in Langmuir films at the air−water interface.[40] Figure 10 shows also that isomerization of multilayer films proceeds at similar rate than in monolayer films in the early stage of the reaction. It gradually decelerates, and finally the rate becomes slower than in monolayer films. Similar behavior was observed in azopolymers in terms of temperature, where only one first-order rate constant is required to accommodate the kinetics in polymers above their glass transition temperature but two are needed in the glassy state. These two different behaviors have been ascribed to differences in the free volume distribution and local structural relaxations in the two phases.[41−45] The kinetics of the thermal cis−trans isomerization in PAzPy multilayer films could be fitted satisfactorily to the equation[46,47]

$$\frac{(Y_{app})_t}{(Y_{app})_0} = \alpha \exp(-k_1 t) + (1 - \alpha) \exp(-k_2 t) \qquad (3)$$

where k_1 and k_2 are the rate constants for the faster and slower components of isomerization, respectively, and α is the fraction of the faster component. According to the obtained kinetic parameters, collected in Table 3, we propose two different first-order isomerization processes. On the one hand, when the free

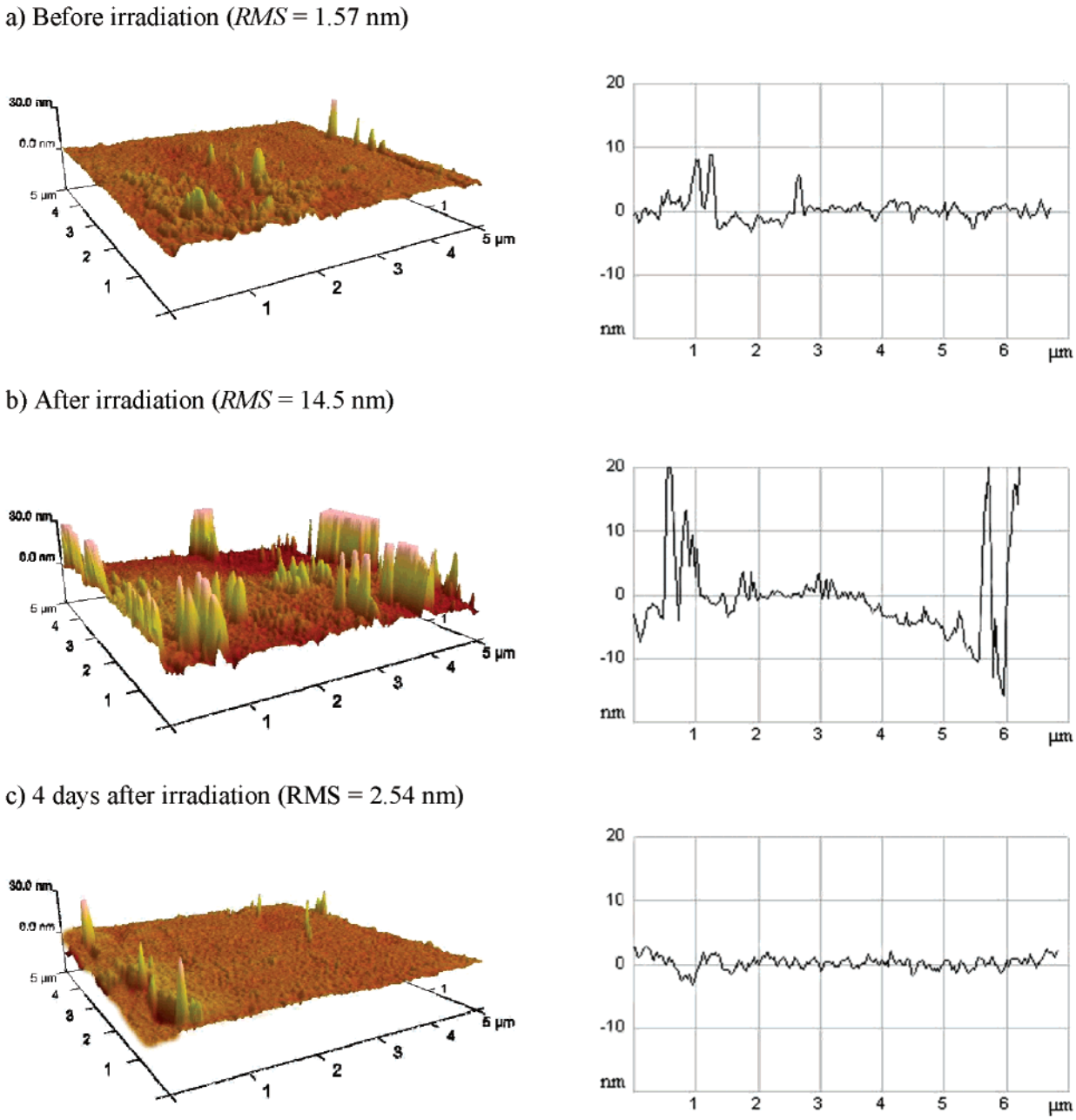

Figure 13. 3D and section analysis AFM images of the 35-layer film transferred at 15 mN m^{-1}: (a) before irradiation with UV light (365 nm), (b) after irradiation, and (c) 4 days after the irradiation process.

volume in the vicinity of an azobenzene is below a critical limit, the cis isomers in such sites are "stressed" and have great propensity to return to the trans form.[42,48,49] The rate of this process is similar that thermal cis−trans isomerization in monolayers, so we determine α and k_2 maintaining k_1 as a constant with the same value obtained for the 1-layer films. The fraction of cis molecules that isomerize following this "fast" kinetics in the films of 1 layer is 1 and decreases with the number of layers. On the other hand, the second process is governed by k_2, which is 1−2 orders smaller than the rate constant of thermal cis−trans isomerization of the azopolymer in solution and k_1. This "slow" process can be related to the strong interactions between cis isomers and surrounding molecules.[39] The fraction of cis molecules that isomerize "slowly" is significant in multilayer films.

To summarize, the photochemical behavior of PAzPy in LB films in terms of film thickness can be classified in three types:

(i) In the monolayer films, the apparent extent of photoisomerization in the photostationary state is around 25%, a percentage much smaller than in solution owing to the more restrictive steric interactions in the ordered structure of the film than in solution. The thermal cis−trans isomerization follows one first-order kinetic, like in solution.

(ii) The films of 5, 10, and 20 layers have very small values of Y_{app} in the photostationary state, indicating that few sites with the free volume necessary to accommodate cis isomers can be created during photoisomerization process in the structure of the multilayer films. Once the sites capable to accommodate cis isomers are formed in the films, the thermal cis−trans isomerization follows two different first-order processes: a fast one ascribed to molecules in more stressed states and a slow kinetics for cis molecules that interact attractively with the neighbor molecules.

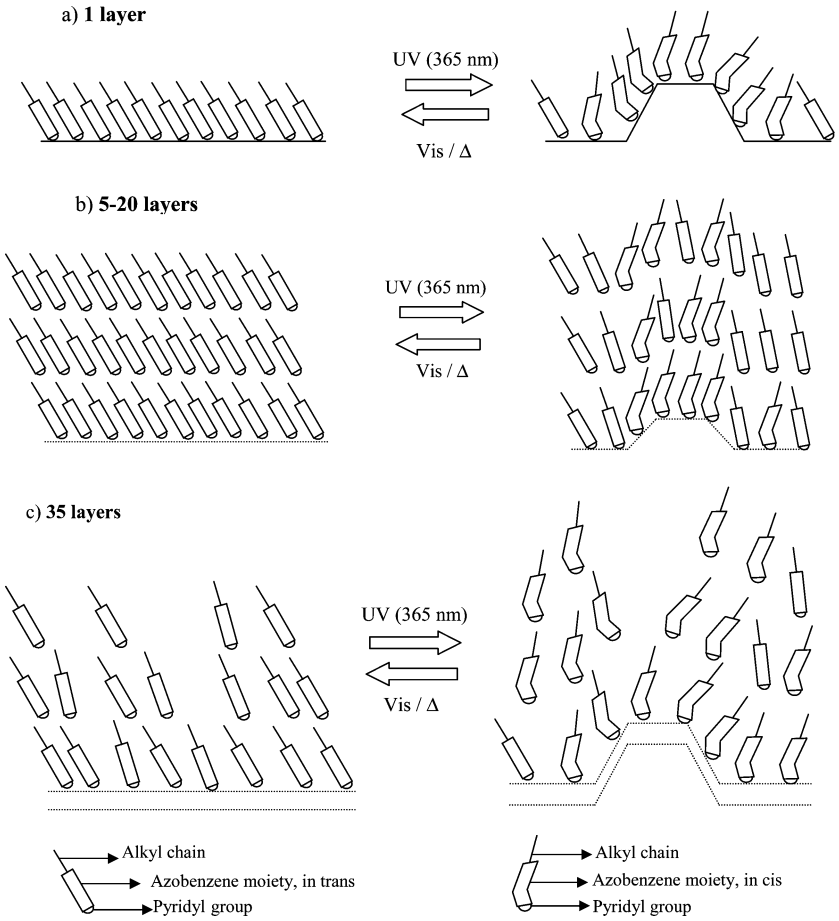

Figure 14. Model of the structural changes of (a) single-layer, (b) multilayer LB films with important degree of order (in our case, films with 5−20 layers), and (c) multilayer LB films where the ordered structure is partially lost, especially in the upper layers (in our case, 35-layer LB films).

(iii) The apparent extent of photoisomerization in the LB films of 35 layers is very high with respect to the thinner films, indicating lower steric restrictions. Furthermore, the thermal cis−trans process is the slowest (hours), indicating that attractive interactions between cis isomers and surrounding molecules are favored in these films.

AFM Microscopy. Isomerization processes were monitorized by AFM in order to obtain insightful information. Some representative results are illustrated in Figures 11, 12, and 13 which show the three-dimensional and section analysis pictures for 1-, 10-, and 35-layer PAzPy LB films transferred at a constant surface pressure of 15 mN m^{-1} onto mica. Each figure shows the surface morphology of the sample (a) before being irradiated with UV light (365 nm), (b) just after the irradiation, and (c) 4 days after the irradiation and indicates the rms roughness. The images were registered in different points of the sample to check the reproducibility of the obtained images.

The rms roughness increases drastically in the films of 1 and 35 layers when the samples are irradiated (from 0.10 to 0.92 nm in the case of the monolayer film and from 1.57 to 14.5 nm in the multilayer film). Moreover, the morphology changes significantly as can be seen in Figures 11b and 13b. There are a number of hills on the surface, whose base and height increase from the monolayer to the 35-layer film. (The width of the hill base is around 150 nm and the height ca. 2.5 nm for the monolayer, and these values increase to ca. 300 and 25 nm for the film of 35 layers.) Meanwhile, in the film of 10 layers slight morphological changes and small increase of rms value (from 0.70 to 1.11 nm) can be observed. Four days after irradiation the hills practically disappear in the films of 1 and 35 layers, and the morphology remains unchanged in the film of 10 layers. The process was repeated several times for the three samples, and the same morphological changes were observed. The reversibility of the morphological changes suggests that after UV irradiation the LB films should maintain a degree of order in the structure of the layers. Similar hills were reported previously in LB films of azobenzene[21,22,24] and interpreted by the following explanation: when the film is irradiated, the azobenzene units start to trans−cis photoisomerize; this process is accompanied by a cross-sectional increase, and then high pressure inside each layer is produced. The stress can be relaxed by the curvature of the layers giving the observed hills.[24]

4. Discussion

Taking into account the above-mentioned results, we propose three different schemes to explain the observed behaviors in terms of structural changes. Figure 14 shows the models for the LB films of 1 (a), 5−20 (b), and 35 layers (c). In the schemes instead of the polymer we show the lateral chains as single molecules for clarity purposes.

The schemes on the left side of the figure represent the LB films before irradiation. The successive vertical transferences produce films with high degree of molecular order in each layer when few layers are deposited. The organization relaxes with the increasing the number of transferences, appearing some little defects in the films of 10 and 20 layers (as Figure 5 shows). The number and size of defects increase with the number of transferences, and some domains where structural order is lost can be seen in the film of 35 layers. The trans molecules are well packed in the first transference as the scheme of the

monolayer shows. A relatively high degree of order is maintained in multilayer films with 20 or fewer layers so the scheme that represents these films is three layers where the molecules are well packed, although some relax in molecular architecture was observed. Further transferences reduce the molecular order of the successive deposited layers in the films. For this reason, the situation of the 35-layer LB film (especially in the upper layers) is illustrated by three layers where the molecules are not well packed.

The schemes on the right part of Figure 14 illustrate the LB films with molecules in the cis form after being irradiated with UV light. As was explained in AFM microscopy section, the trans−cis photoisomerization gives rise to an increase in cross-sectional area of azobenzenes that produces a great stress inside the layers. This stress can be released by giving curvature to the film in a three-dimensional morphological change.[24] These curvatures are relatively easy to form in monolayer films where upper layers that can exert pressure in the opposite direction of the curvature do not exist (Figure 13a). Once the UV radiation stops, the cis molecules are not stable in the formed hills, probably due to the constrained conformation,[42] and isomerize into trans form quickly. The hills formation is more hindered in the films of 5−20 layers (Figure 13b) where a relatively high degree of organization exists, particularly in the film of 5 layers. When one layer curves to accommodate cis isomers, the upper layers, with the molecules well-packed, try to hinder this curvature to conserve their intrinsic order. Consequently, photoisomerization of the chromophores is very inhibited, and the apparent extent of photoisomerization is very small at the photostationary state. Nevertheless, once the photostationary state is reached, cis isomers can interact with surrounding molecules of the upper layers, and this can explain the slow kinetic component in the thermal cis−trans isomerization. In the case of the 35-layer film (Figure 13c), the LB film has lost part of the molecular order in the upper layers, and the curvature of the layers should be relatively easy in these domains, and then azobenzene units can isomerize, but this phenomenon cannot explain the huge increase of the Y_{app} values in these films. The relatively high Y_{app} obtained values can be related with the cooperative motions that exist between azobenzene units; therefore, the formation of hills in the upper layers can favor the curvature of the lower ones, and the azobenzene units can photoisomerize easily as consequence of lower spatial restrictions. With respect to the thermal cis−trans kinetics, this process is exceptionally slow considering that PAzPy behaves as an aminoazobenzene. This phenomenon may be interpreted as a result of the greater number of attractive interactions between cis isomers and surrounding molecules occurring in 35-layer films, and then a greater number of cis molecules follows the slow kinetics in the cis−trans isomerization.

With respect to the chromophore surface density, this factor does not affect significantly the apparent extent of photoisomerization, as Table 2 shows. Nevertheless, the two rate constants of the thermal cis−trans isomerization diminish significantly with the increase of transference surface pressure (Table 3), probably because interactions between cis isomers and surrounding molecules are favored.

5. Conclusions

This paper shows the investigation of trans−cis photoisomerization extent in the photostationary state and thermal cis−trans isomerization kinetics of an azopolymer incorporated into an organized structure such as a Langmuir−Blodgett film in terms of film thickness and chromophore surface density. Furthermore, the morphological changes during photoisomerization process were monitored by AFM.

Photoisomerization of PAzPy molecules in the fabricated LB films produces three-dimensional structure changes of the films due to the cross-section increase during trans−cis transformation. The three-dimensional structures in the photostationary state may be ordered structures which can explain the reversibility of the morphological changes observed by AFM. The apparent extent of photoisomerization is related to the facility of the 2-dimensional films to be curved, giving ordered three-dimensional structures that hold cis isomers. This deformation of the film depends on the number of layers with well-ordered structure. When the number of well ordered layers increases, Y_{app} diminishes. As the number of transferences increases, the deposition of layers became worse and then the layers are more disordered; consequently, the apparent extent of photoisomerization increases because curvature of these layers is easier in the defects. The chromophore surface density practically does not affect the obtained Y_{app} values at the photostationary state.

Thermal cis−trans isomerization kinetics depends on both film thickness and chromophore surface density. Cis isomers are converted to the trans form quickly in the monolayer films, following a first-order kinetics. Nevertheless, when more than one layer is transferred, two first-order processes are needed to explain the experimental results. One term corresponds to the fraction of cis isomers that are transformed at a similar rate as in the monolayer films. The other term should be related to the cis isomers that are attractively interacting with neighbor molecules; the interactions are favored with the number of layers and chromophore surface density.

Acknowledgment. The authors thank Dr. Serrano and Dr. Oriol from Universidad Zaragoza for the synthesis of PAzPy. The authors appreciate very much both Jordi Diaz's and Ismael Diez's efforts in the AFM measurements. Finally, we are grateful for financial assistance from the project of Ministerio de Educación y Ciencia (BQU2003-01765). M. Haro and B. Giner gratefully acknowledge their FPU and FPI fellowships from Ministerio de Educación y Ciencia.

References and Notes

(1) Natansohn, A.; Rochon, P. *Chem. Rev.* **2002**, *102*, 4139.
(2) Frese, T.; Wendorff, J. H.; Janietz, D.; Cozan, V. *Chem. Mater.* **2003**, *15*, 2146.
(3) El Halabieh, R. H.; Mermut, O.; Barrett, C. J. *Pure Appl. Chem.* **2004**, *76*, 1445.
(4) Oliveira, O. N., Jr.; Dos Santos, D. S., Jr.; Balogh, D. T.; Zucolotto, V.; Mendonça, C. R. *Adv. Colloid Interface Sci.* **2005**, *116*, 179.
(5) Eich, M.; Wendorff, J. *Makromol. Chem.* **1987**, *8*, 467.
(6) Rodríguez, F. J.; Sánchez, C.; Villacampa, B.; Alcalá, R.; Cases, R.; Millaruelo, M.; Oriol, L.; Lörincz, E. *Opt. Mater.* **2006**, *28*, 480.
(7) Ichimura, K.; Suzuki, Y.; Seki, K.; Hosoki, K.; Aoki, K. *Langmuir* **1988**, *4*, 1214.
(8) Advincula, R. C.; Park, E.; Baba, A.; Kaneko, F. *Langmuir* **2003**, *19*, 654.
(9) Rau, H. *Photochemistry and Photophysics*; Rabek, J. K., Ed.; CRC Press: Boca Raton, FL, 1990.
(10) Xie, S.; Natansohn, A.; Rochon, P. *Chem. Mater.* **1993**, *5*, 403.
(11) Sudesh, Kumar, G.; Neckers, D. C. *Chem. Rev.* **1989**, *89*, 1915.
(12) Matsumoto, M.; Terrettaz, S.; Tachibana, H. *Adv. Colloid Interface Sci.* **2000**, *87*, 147.
(13) Conroy, M.; Ali-Adib, Z.; Hodge, P.; West, D.; King, T. *J. Mater. Chem.* **1994**, *4*, 1.
(14) Ulman, A. *An Introduction to Ultrathin Organic Films: From Langmuir-Blodgett to Self-Assembly*; Academic Press: San Diego, 1991.
(15) Oliveira, O. N., Jr.; Raposo, M.; Dhanabalan, A. *Langmuir-Blodgett (LB) and Self-Assembled Polymeric Films*; Academic Press: New York, 2001.

(16) Tachibana, H.; Nakamura, T.; Matsumoto, M.; Komizu, H.; Manda, E.; Niino, H.; Yabe, A.; Kawabata, Y. *J. Am. Chem. Soc.* **1989**, *111*, 3080.
(17) Seki, T.; Tamaki, T.; Suzuki, Y.; Kawanishi, Y.; Ichimura, K. *Macromolecules* **1989**, *22*, 3505.
(18) Matsumoto, M.; Tachibana, H.; Sato, F.; Terrettaz, S. *J. Phys. Chem. B* **1997**, *101*, 702.
(19) Tachibana, H.; Azumi, R.; Tanaka, M.; Matsumoto, M.; Sako, K.; Sakai, H.; Abe, M.; Kondo, Y.; Yoshino, N. *Thin Solid Films* **1996**, *284*, 73.
(20) Geue, T.; Stumpe, J.; Pietsch, U.; Haak, M.; Kaupp, G. *Mol. Cryst. Liq. Cryst.* **1995**, *262*, 157.
(21) Velez, M.; Mukhopadhyay, S.; Muzikante, I.; Matisova, G.; Vieira, S. *Langmuir* **1997**, *13*, 870.
(22) Seki, K.; Kojima, K.; Ichimura, K. *J. Phys. Chem. B* **1999**, *103*, 10338.
(23) Seki, T.; Koyima, J.; Ichimura, K. *Macromolecules* **2000**, *33*, 2709.
(24) Matsumoto, M.; Miyazaki, D.; Tanaka, M.; Azumi, R.; Manda, E.; Kondo, Y.; Yoshino, N.; Tachibana, H. *J. Am. Chem. Soc.* **1998**, *120*, 1479.
(25) Haro, M.; Ross, D. J.; Oriol, L.; Gascón, I.; Cea, P.; López, M. C.; Aroca, R. F. *Langmuir*, in press (doi: 10.1021/la061491p).
(26) Royo, F. M.; López, M. C.; Ruiz, B.; Camacho, A.; Lozano, J. M.; Urieta, J. *Rev. Acad. Cienc. Exactas, Fis., Quim. Nat. Zaragoza* **1993**, *48*, 177.
(27) Roberts, G. *Langmuir-Blodgett Films*; Plenum Press: New York, 1990.
(28) Cea, P.; Morand, J. P.; Urieta, J. S.; López, M. C.; Royo, F. M. *Langmuir* **1996**, *12*, 1541.
(29) Cea, P.; Lafuente, C.; Urieta, J. S.; López, M. C.; Royo, F. M. *Langmuir* **1997**, *13*, 4892.
(30) Martín, S.; Cea, P.; Lafuente, C.; Royo, F. M.; López, M. C. *Surf. Sci.* **2004**, *563*, 27.
(31) Allinger, L. *J. Am. Chem. Soc.* **1977**, *99*, 8127.
(32) Pedrosa, J. M.; Martín, M. T.; Camacho, L.; Möbius, D. *J. Phys. Chem. B* **2002**, *106*, 2583.
(33) Porter, M. D.; Bright, T. B.; Allara, D. L. *J. Am. Chem. Soc.* **1987**, *109*, 3559.
(34) Byrd, H.; Whipps, S.; Pike, J. K.; Ma, J.; Nagler, S. E.; Talham, D. R. *J. Am. Chem. Soc.* **1994**, *116*, 295.
(35) Kajiyama, T.; Aizawa, M. *New Developments in Construction and Functions of Organic Thin Films*; Elsevier: Amsterdam, 1996.
(36) Shimomura, M.; Kunitake, T. *J. Am. Chem. Soc.* **1987**, *109*, 5175.
(37) Matczyszyn, K.; Bartkowiak, W.; Leszczynski, J. *J. Mol. Struct.* **2001**, *565*−*566*, 53.
(38) Srikhirin, T.; Laschitsch, A.; Neher, D.; Johannsmann, D. *Appl. Phys. Lett.* **2000**, *77*, 963.
(39) Mechau, N.; Saphiannikova, M.; Neher, D. *Macromolecules* **2005**, *38*, 3894.
(40) Zhuang, X.; Lackritz, H. S.; Shen, Y. R. *Chem. Phys. Lett.* **1995**, *246*, 279.
(41) Priest, W. J.; Sifain, M. M. *J. Polym. Sci., Polym. Chem. Ed.* **1971**, *9*, 3161.
(42) Paik, C. S.; Morawetz, H. *Macromolecules* **1972**, *5*, 171.
(43) Eisenbach, C. D. *Makromol. Chem.* **1978**, *179*, 2489.
(44) Eisenbach, C. D. *Makromol. Chem., Rapid Commun.* **1980**, *1*, 287.
(45) Mita, I.; Horie, K.; Hirao, K. *Macromolecules* **1989**, *22*, 558.
(46) Imai, Y.; Naka, K.; Chujo, Y. *Macromolecules* **1999**, *32*, 1013.
(47) Wang, C.; Weiss, R. G. *Macromolecules* **2003**, *34*, 3833.
(48) Haitjema, H. J.; Morgan, G. L. V.; Tan, Y. Y.; Challa, G. *Macromolecules* **1994**, *27*, 6201.
(49) Grebenkin, S. Y.; Bolshakov, B. V. *J. Polym. Sci., Part B: Polym. Phys.* **1999**, *37*, 1753.

MA0624752